

Article

# Assessment Method Based on AIS Data Combining the Velocity Obstacle Method and Pareto Selection for the Collision Risk of Inland Ships

Yan Wang , Yi Zhang, Hengchao Zhao and Hongbo Wang \* 

State Key Laboratory on Integrated Optoelectronics, College of Electronic Science and Engineering, Jilin University, Changchun 130012, China

\* Correspondence: wang\_hongbo@jlu.edu.cn; Tel.: +86-0431-8516-8270

**Abstract:** A ship collision risk assessment model is an essential part of ship safety navigation. At present, the open water collision risk assessment model (such as the closest point of approach) is applied, but a ship collision risk model suitable for inland rivers is still in the exploration stage. Compared with open waters, the inland waterway has a larger density of ships, and the land and water environments are complex. The existing risk assessment models lack adaptability under the conditions of inland navigation. Therefore, this paper proposes a real-time collision risk assessment method for ships navigating inland rivers. This method utilizes the information of ships' size in the automatic identification system (AIS) to construct the velocity obstacle cone between convex polygonal targets using the velocity obstacle method. Then, according to the geometric relationship between the relative velocity of two targets and the velocity obstacle cone, a new collision risk assessment model is defined. This model defines two indicators to evaluate the navigation collision risk: the degree of velocity obstacle intrusion (DVOI) and time of velocity obstacle intrusion (TVOI). These two indicators assess the risk of collision, respectively, from two aspects speed and course. In addition, a method using a trajectory compression algorithm to screen collision avoidance operation points in ship AIS trajectory is proposed to screen collision avoidance scenarios in the Yangtze River waterway. The effectiveness of the proposed collision risk model is verified in course-keeping and collision avoidance scenarios and compared with the traditional closest point of approach (CPA) method. The results indicate that the evaluation model for collision risk assessment is more accurate than the CPA method in all scenarios. Finally, this paper uses the Pareto selection algorithm to combine DVOI and TVOI, which can identify the ship that poses the greatest risk to our ship.

**Keywords:** risk assessment; inland ships; velocity obstacle; AIS data; Pareto selection; closest point of approach



**Citation:** Wang, Y.; Zhang, Y.; Zhao, H.; Wang, H. Assessment Method Based on AIS Data Combining the Velocity Obstacle Method and Pareto Selection for the Collision Risk of Inland Ships. *J. Mar. Sci. Eng.* **2022**, *10*, 1723. <https://doi.org/10.3390/jmse10111723>

Academic Editors: Mohamed Benbouzid, Anne Blavette and Nicolas Guillou

Received: 7 October 2022

Accepted: 8 November 2022

Published: 11 November 2022

**Publisher's Note:** MDPI stays neutral with regard to jurisdictional claims in published maps and institutional affiliations.



**Copyright:** © 2022 by the authors. Licensee MDPI, Basel, Switzerland. This article is an open access article distributed under the terms and conditions of the Creative Commons Attribution (CC BY) license (<https://creativecommons.org/licenses/by/4.0/>).

## 1. Introduction

Inland river shipping ensures the stability and smooth flow of the logistics supply chain and is an important part of a comprehensive transportation system [1]. Compared with land transportation, inland river shipping is a more environmentally friendly means of transportation. Increasing the proportion of inland river shipping in cargo transportation is of great importance to achieve carbon neutralization and energy conservation. However, the complex navigation conditions and crowded traffic conditions of inland river sections have been the biggest external factors that restrict the intellectualized navigation of inland river vessels [2]. The most significant difference between inland navigation and open water is the increase in ship density. These characteristics challenge the establishment of a navigation risk model for inland ships.

At present, no method for the collision risk assessment of inland waterways has been widely adopted. However, it is very important to have an effective collision risk assessment model for ship-assisted collision avoidance or intelligent navigation technology. The model

can provide a basis for decision-making algorithms to select appropriate collision avoidance and resumption timing, as well as an appropriate collision avoidance method. In addition, the collision risk assessment module needs to run continuously throughout the algorithm. Therefore, it is necessary for ship-assisted collision avoidance or the intelligent navigation technology of ships to realize an effective risk assessment method suitable for inland ships.

Navigation risk is a very broad term. Many factors may lead to the navigation risk of ships, such as environmental impact (weather, etc.), the impact of mechanical equipment, and human factors [3]. However, man-made factors are generally recognized by scholars as the biggest factor that causes the navigation danger to ships [3–6]. In the course of navigation, human factors are mainly reflected in three parts: trajectory prediction, collision risk detection, and collision avoidance strategies [7]. Collision risk detection is the research issue of this paper. At present, research in this area has two directions, one of which is to study the collision risk of an area. For example, Liu et al. obtained clusters by clustering and then computed the collision risk for all clusters to obtain regional collision risk values [8]. Kang et al. employed the weighted least squares method to derive speed–density formulas for ships in the Singapore Strait [9]. These results can be utilized to describe the traffic characteristics of certain navigation sections, such as inland rivers, but can only be used as a reference, not for the actual ship navigation collision risk detection. The other direction is to directly study the collision risk values between ships, usually based on expert knowledge or probability. The following is an introduction to two research methods in this direction.

The most widely used method is the closest point of approach (CPA), of which two indicators, the distance of CPA (DCPA) and time of CPA (TCPA), need to be determined by expert knowledge. Mou et al. used a linear regression model to determine the correlation between CPA parameters and ship size, speed, and course in the European port of Rotterdam [10]. Kang et al. asked eight captains with more than 10 years of work experience to acquire data from simulated laboratory voyages in order to obtain CPA index thresholds in restricted waters [11]. However, the CPA method is only a simple estimation and is not applicable in many situations because the size information of the ship is ignored [12], which is especially true in inland waterways. The collision risk assessment model based on the ship domain is also a widely studied scheme. The ship domain cannot directly quantify the risk value. Szlapczynski proposed the proximity factor index, which was the earliest application of the ship domain to the collision risk assessment model [13]. On this basis, two indicators—the degree of domain violation and time to domain violation—were proposed [14]. The degree of overlap in the area of ship domains is also an indicator of risk calculation [7,12,15–19]. However, the domain radius of a ship is often several times the length of its own ship when considering maneuverability [20,21]. This feature makes it difficult to apply to high-density ship scenarios, especially in inland waterways where the lane separation system is implemented. Some scholars have proposed new indicators or combined other means with the methods based on expert knowledge. Liu et al. proposed a new collision risk indicator based on ship maneuverability and ship domain-danger sector; this indicator defines the collision risk according to the optional range of heading [22,23]. You et al. proposed a new collision risk index, namely virtual intrusion, based on ship maneuverability and collision avoidance rules [24]. Li et al. proposed a new collision risk assessment model based on the relative course selection range by combining the velocity obstacle method with the ship domain [25]. Chen et al. combined the velocity obstacle method with the CPA method, first using the velocity obstacle method to select the target ship, and then using the CPA method to calculate the risk [26]. Most of these methods consider only the course for collision risk assessment while ignoring the speed when applying the velocity obstacle method. Furthermore, the use of fuzzy logic [15,16,27], neural network [28], and evidential reasoning [29,30] methods to take various indicators into careful consideration is a hot research direction. These achievements are of positive significance for promoting the establishment of a collision risk model. However, they are usually utilized in open water only, and few studies are conducted on the assessment of collision risk of inland ships.

Research on the probability-based collision risk model has been previously conducted [31]. The use of Bayesian networks [6,32,33] to infer collision risk probability models is a research hotspot in this field. Cai et al. proposed a risk degree model weighted by indicators based on the principle of information entropy [34]. Mujeeb-Ahmed et al. used Latin hypercube sampling technology to generate 50 expected collision scenarios in order to study the collision risk assessment model of offshore supply ships for offshore facilities [35]. However, obtaining an accurate probability density function is often the premise for the application of such methods.

In a word, the current research direction of the risk model shows the characteristics of multimethod fusion, and both empirical and probability-based models pay more attention to the use of automatic identification system (AIS) information [19,26,32,34,36,37]. However, the current threshold settings for risk assessment indicators (such as CPA) are not directional; thus, it is not possible to determine the threshold in a waterway based on expert knowledge. Whereas probability-based collision avoidance is not sufficiently reliable, a reliable collision risk assessment model that can be applied to inland rivers is still lacking. In this paper, on the basis of the AIS size data of ships, a navigation collision risk assessment model for inland rivers is proposed based on the velocity obstacle method and Pareto selection. In the proposed model, two collision risk indicators—the degree of velocity obstacle intrusion (DVOI) and time of velocity obstacle intrusion (TVOI)—are obtained using the velocity obstacle method, assessing the collision risk of navigation from the two aspects of course and speed, respectively. Finally, the most dangerous ships to the current navigation are obtained using the Pareto selection method. The following text is arranged as follows: Section 2 introduces the construction method of the velocity obstacle zone and the calculation method of DVOI and TVOI. Section 3 discusses how to filter collision avoidance situations in AIS data using a compression algorithm and to use the Pareto selection method with a threshold. Section 4 introduces the data preprocessing and the main flow of the algorithm. Section 5 uses AIS data in the real navigation process to evaluate the collision risk of three different ship navigation scenarios using the DVOI/TVOI and CPA methods simultaneously and compares them. The combination of DVOI/TVOI and Pareto selection with a threshold can determine the ships that are currently the most threatening to our ship. Section 6 summarizes of the full text.

## 2. Calculation of DVOI and TVOI

The velocity obstacle method was first proposed by Fiorini et al. and applied to the path planning of robots in dynamic environments [38]. To avoid the problem of turning, a circle is used to represent the shape of the robot, the radius of robot  $A$  is superimposed onto robot  $B$ , and the velocity obstacle cone  $CC_{A,B}$  is obtained, as presented in Figure 1a, where  $\lambda_r$  and  $\lambda_f$  are two tangent lines passing through point and circle respectively. The radius of circle  $B$  is the sum of  $R_A$  and  $R_B$ , which are the radii of robot  $A$  and robot  $B$ , respectively. The collision can be avoided by selecting appropriate  $\vec{V}_A$  so that the direction of relative velocity  $\vec{V}_{A,B}$  falls outside of  $CC_{A,B}$ .

The width of inland ships is limited due to the limited channel width. To ensure cargo capacity, the ship shape is closer to a cuboid. The length and width of the ships in AIS data were used to model the ship shape with a rectangle, and the velocity obstacle cone in Figure 1b was obtained by building the velocity obstacle method. The ship filled with vertical lines is our ship, which is represented by  $O$ , and the ship filled with grid lines is the target ship, which is represented by  $T$ . The specific method is introduced in Section 2.1.

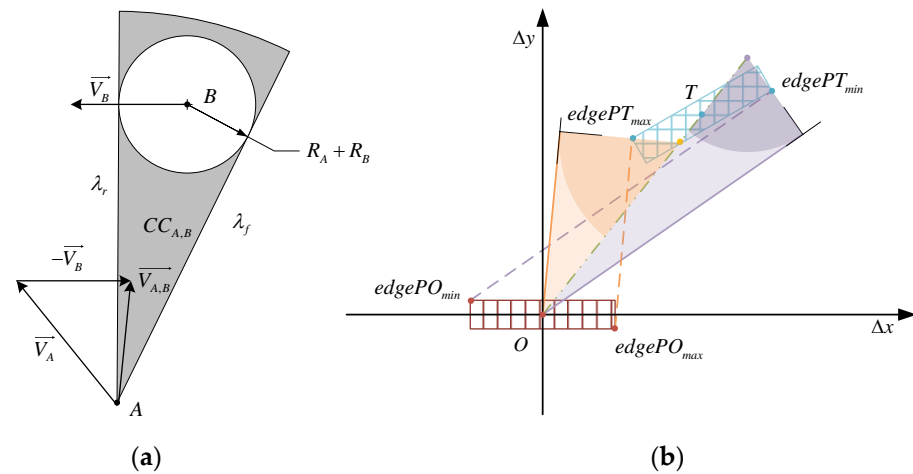


**Figure 1.** Schematic of the velocity obstacle. (a) Velocity obstacle for robots, (b) velocity obstacle for inland ships.

2.1. Structure Velocity Obstacle Cone

An AIS can provide real-time ship navigation information [36], including longitude, latitude, course, speed, and ship size. For ship size modeling, the longitude and latitude need to be mapped to the relative position coordinate system, as presented in Figure 1b. According to Equations (1) and (2), the relative distance coordinate  $(x_{map}, y_{map})$  between the longitude and latitude  $(\lambda_{target}, \varphi_{target})$  of the target point  $P_{target}$  and the longitude and latitude  $(\lambda_{ori}, \varphi_{ori})$  of the reference point  $P_{ori}$  can be obtained.

$$\begin{cases} x_{map} = r_{orilat} \times \Delta\lambda \\ y_{map} = r_{orilon} \times \Delta\varphi \end{cases} \tag{1}$$

$$\begin{cases} r_{orilat} = \frac{a_e \cos \varphi_{ori}}{(1 - e_1^2 \sin^2 \varphi_{ori})^{\frac{1}{2}}} \\ r_{orilon} = \frac{a_e (1 - e_1^2)}{(1 - e_1^2 \sin^2 \varphi_{ori})^{\frac{3}{2}}} \end{cases} \tag{2}$$

where the radius of weft circle  $r_{orilat}$  is  $N(\varphi_{ori}) \cos \varphi_{ori}$ , and the radius of warp circle  $r_{orilon}$  is  $M(\varphi_{ori})$ .  $\Delta\lambda$  and  $\Delta\varphi$  are the longitude and latitude differences of the target’s relative reference point, respectively. Equations (3) and (4), respectively, provide the radius of curvature of the meridian circle and prime vertical circle at reference point  $P_{ori}$ .

$$M(\varphi) = \frac{a_e (1 - e_1^2)}{(1 - e_1^2 \sin^2 \varphi)^{\frac{3}{2}}} \tag{3}$$

$$N(\varphi) = \frac{a_e}{(1 - e_1^2 \sin^2 \varphi)^{\frac{1}{2}}} \tag{4}$$

The WGS84 coordinate system was adopted here, and ellipsoidal parameters are presented in Table 1, where  $e_1^2$  is the first eccentricity,  $e_1^2 = \frac{a_e^2 - b_e^2}{a_e^2}$ .

**Table 1.** Ellipsoid parameters of WGS84.

Major Semi-Axis $a_e(m)$	Minor Semi-Axis $b_e(m)$	Flattening $f_e$
6,378,137	6,356,752.314	1:298.257223563

The ship in navigation is represented by a rectangle, and the ship domain is represented by four vertices (upper left, upper right, lower right, lower left). The relative distance

coordinate  $(x, y)$  corresponding to the longitude and latitude of the ship is taken as the center point coordinate of the ship. According to the geometric relationship, the coordinates of the four vertices can be obtained using Equation (5).

$$\begin{cases} (x_{fl}, y_{fl}) = (x + x_{fm} + dx_{fl}, y + y_{fm} + dy_{fl}) \\ (x_{fr}, y_{fr}) = (x + x_{fm} + dx_{fr}, y + y_{fm} + dy_{fr}) \\ (x_{ar}, y_{ar}) = (x + x_{am} + dx_{ar}, y + y_{am} + dy_{ar}) \\ (x_{al}, y_{al}) = (x + x_{am} + dx_{al}, y + y_{am} + dy_{al}) \end{cases} \quad (5)$$

The ship length obtained from the AIS data is  $l$ , and the width is  $w$ . The heading angle  $\theta_{ori}$  was converted into the included angle  $\phi$  between the ship and the positive direction of the  $x$  - axis using Equation (6) in Figure 2.

$$\phi = \begin{cases} 90^\circ - \theta_{ori} & 0 < \theta_{ori} < 90^\circ \\ 450^\circ - \theta_{ori} & 90^\circ \leq \theta_{ori} \leq 360^\circ \end{cases} \quad (6)$$

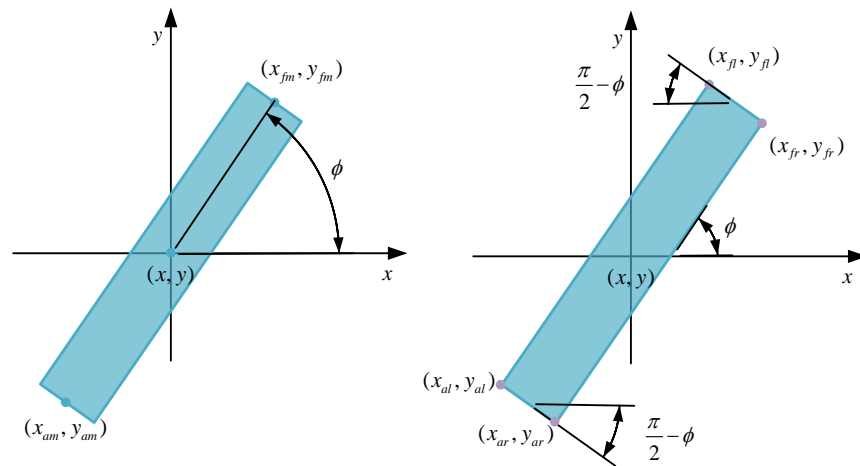


Figure 2. Geometric relationship diagram of ship size model vertices.

$x_{fm}, y_{fm}, x_{am}, y_{am}$  are the abscissa and ordinate of the midpoint of the front and rear ends of the ship, respectively, which can be calculated using Equations (7) and (8).  $dx_{fl}, dx_{fr}, dx_{ar}, dx_{al}$  are the  $x$  - axis direction offsets of the top left, top right, bottom right, and bottom left vertices relative to the midpoint of the front and rear ends, respectively. Similarly, the offset in the  $y$  - axis direction can be calculated using Equations (9) and (10).

$$\begin{cases} x_{fm} = \frac{l}{2} \cos(\phi) \\ y_{fm} = \frac{l}{2} \sin(\phi) \end{cases} \quad (7)$$

$$\begin{cases} x_{am} = \frac{l}{2} \cos(\pi + \phi) \\ y_{am} = \frac{l}{2} \sin(\pi + \phi) \end{cases} \quad (8)$$

$$\begin{cases} dx_{fl} = dx_{al} = \frac{w}{2} \cos(\phi + \frac{\pi}{2}) \\ dy_{fl} = dy_{al} = \frac{w}{2} \sin(\phi + \frac{\pi}{2}) \end{cases} \quad (9)$$

$$\begin{cases} dx_{fr} = dx_{ar} = \frac{w}{2} \cos(\phi + \frac{3\pi}{2}) \\ dy_{fr} = dy_{ar} = \frac{w}{2} \sin(\phi + \frac{3\pi}{2}) \end{cases} \quad (10)$$

The distance mapping is only approximate to the reference point. Thus, when the target point is far from the reference point, a more accurate angular relationship between the two coordinates can be obtained using the Mercator projection, as expressed in Equation (11).

$(x_{mercator}, y_{mercator})$  is the Mercator projection coordinate corresponding to longitude and latitude  $(\lambda, \varphi)$ .

$$\begin{cases} x_{mercator} = a_e \ln\left(\tan\left(45^\circ + \frac{\varphi}{2}\right)\right) \left(\frac{1-e_1 \sin \varphi}{1+e_1 \sin \varphi}\right)^{\frac{e_1}{2}} \\ y_{mercator} = a_e \lambda \end{cases} \quad (11)$$

Unlike the construction method of the velocity obstacle cone in Figure 1a, which uses the tangent point as the critical collision point, a rectangle cannot stack the radius from any direction like a circle. Thus, a method to determine the critical collision point of a convex polygon through the slope is presented here. This paper presents a method to determine the critical collision point by the slope of the line connecting the vertices between convex polygons. As shown in the algorithm in Algorithm 1 first, the relative positions of the two ships are judged. For example, the distance from all vertices of our ship to the  $y$ -axis is greater than that from any vertex of the target ship to the  $y$ -axis. In the scenario presented in Figure 3, the only necessary task is to connect our ship to the vertices of the target ship. The two lines with the largest and smallest slopes are tangent lines, and the four vertices of these two lines are edge collision points. The velocity obstacle cone between convex polygons can be constructed by passing through the center point of our ship and making two rays parallel to these two straight lines. When the distance from the target ship's vertex to the  $y$ -axis is smaller than that from our ship's vertex to the  $y$ -axis, that is, as presented in Figure 4a, if the wrong velocity obstacle cone obtained according to the aforementioned method, then all points will be rotated  $90^\circ$  clockwise with the origin as the center point, and then the critical impact point will be determined using the aforementioned method and the velocity obstacle cone obtained, as presented in Figure 4b. Then, the points will be rotated  $90^\circ$  counterclockwise to obtain the original coordinates of the critical impact point and calculate the true slope, thus obtaining the correct velocity obstacle cone (Figure 4c).

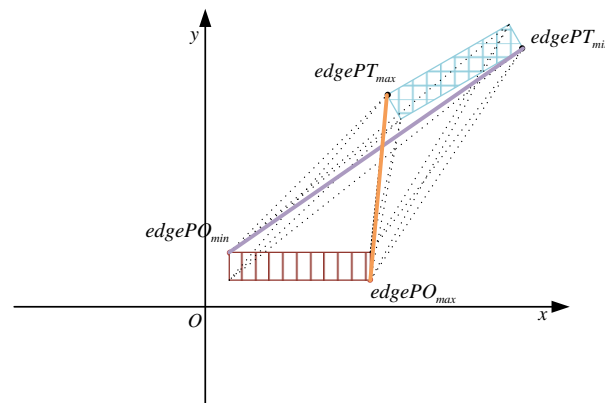
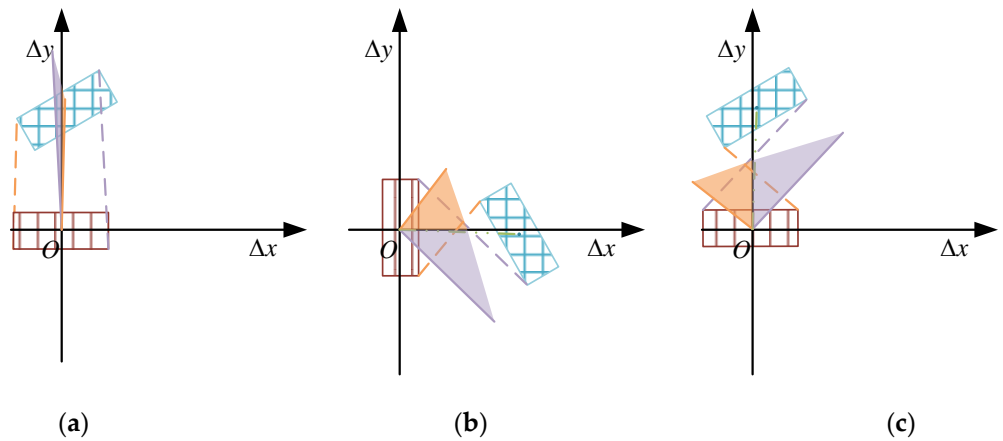
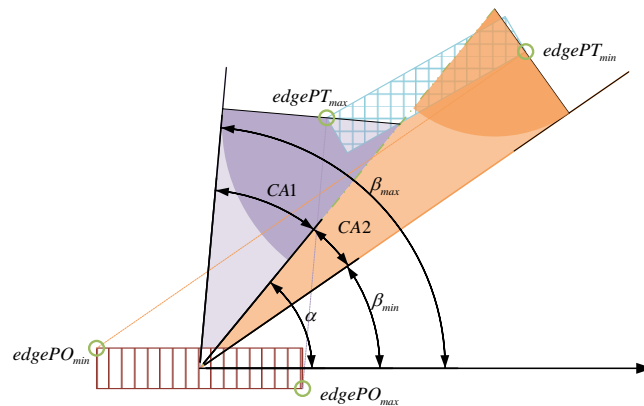


Figure 3. Selecting the critical collision point by slope (scenario 1).



**Figure 4.** Selecting the critical collision point by slope (scenario 2). (a) The algorithm 1 was directly used in this scenario and obtained the wrong velocity obstacle cone. (b) After the vertices of the two ships rotated 90° clockwise around the origin, the velocity obstacle cone was obtained through algorithm 1. (c) shows (b) rotated 90 ° counterclockwise.

Finally, the velocity obstacle cone under the polar coordinate system was obtained as presented in Figure 5, where  $\alpha$  is the included angle of the connecting line between the center points of the two ships, and  $\beta_{min}$ ,  $\beta_{max}$  are the included angles between the line with the minimum and maximum slopes of the connecting line among the vertices of the two ships and the polar axis, respectively. CA1 and CA2 are the center angles corresponding to the two velocity obstacle cones, respectively. The value of  $\alpha$ ,  $\beta_{min}$ ,  $\beta_{max}$ , CA1, CA2 is within zero and  $2\pi$ .



**Figure 5.** Velocity obstacle cone of the target ship in polar coordinates.

Algorithm 1. Algorithm for selecting critical collision points by slope (where, Input is the vertex of our ship and the target ship, and the number of vertices of the polygon;  $PT(2)$  represents the ordinate of the vertex of the target ship;  $CWO90$  and  $CCWO90$  are subfunctions that rotate the point 90° clockwise and 90° counterclockwise about the origin, respectively;  $K$  is a one dimensional vector that stores all slopes;  $indexMax$  and  $indexMin$  are the subfunctions to obtain the maximum and minimum position indices, respectively; and  $Round$  is the downward rounding function).

---

**Algorithm 1:** Select critical collision point by slope

---

**Input:**  $POs, PTs, PNum, PTs, PNum$

**Output:**  $PO_{min}, PT_{min}, PO_{max}, PT_{max}$

---

```

// Classification according to relative position
1  aroundFlag ← 0;
2  foreach  $PT \in PTs$  do
3    if  $|PT(2)| < Max(|PO(2)|)$  then
4      // Rotate 90 degrees clockwise around the origin
5       $POs \leftarrow CWO90(POs)$ ;
6       $PTs \leftarrow CWO90(PTs)$ ;
7      aroundFlag ← 1;
8      break;
9    end
10  end
// Calculate vertex connection slope
11  $i \leftarrow 1$ ;
12 foreach  $PO \in POs$  do
13   foreach  $PT \in PTs$  do
14      $K(i) \leftarrow slop(PO, PT)$ ;
15      $i \leftarrow i + 1$ ;
16   end
17 end
// Determine the vertex corresponding to the extreme value of the slope
18  $iMax \leftarrow indexMax(K)$ ;
19  $iMin \leftarrow indexMin(K)$ ;
20  $PO_{min} \leftarrow POs(Round(iMin \div PNum))$ ;
21  $PO_{max} \leftarrow POs(Round(iMax \div PNum))$ ;
22  $PT_{min} \leftarrow PTs(iMin \% PNum)$ ;
23  $PT_{max} \leftarrow PTs(iMax \% PNum)$ ;
// Rotate the vertex back to its original position
24 if aroundFlag = 1 then
25    $[PO_{min}, PT_{min}, PO_{max}, PT_{max}] \leftarrow CCWO90(PO_{min}, PT_{min}, PO_{max}, PT_{max})$ ;
26 end

```

---

## 2.2. Calculation of DVOI

DVOI indicates the degree of invasion of our ship into the velocity obstacle cone formed by the target ship. A smaller DVOI corresponds to a lower degree of invasion (approach) of our ship to the velocity obstacle cone of the target ship; that is, the two ships are safer. As presented in Figure 6a, the center angle that corresponds to the velocity obstacle cone is CA1 and CA2, and the boundary line of the two sector areas is the line connecting the center points of the two ships. On the basis of these two sectors, the extension velocity obstacle cone can be obtained by extending  $90^\circ$  respectively in the direction of the connecting line away from the ship's center point, that is, the area corresponding to the central angles CA3 and CA4. The center angle of the area outside the corresponding area CA1, CA2, CA3, CA4 is CA5.

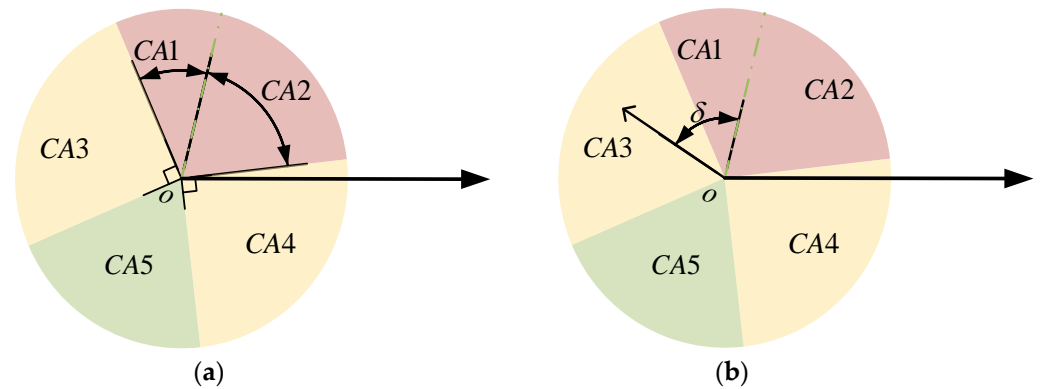


**Figure 6.** Velocity obstacle cone and extended velocity obstacle cone. (a) Velocity obstacle cone and expanded velocity obstacle cone. (b) The angle between the relative velocity direction and the connecting line between the center points of the two ships.

As presented in Figure 6b  $\delta$  denotes the angle between the relative velocity direction and the connecting line between the center points of the two ships, which has a value range within  $[0, \pi]$ . When it falls in the area corresponding to the center angle CA1 or CA2, it indicates that a collision may occur when sailing along the current velocity direction, and the DVOI value is 1. When it falls in the area corresponding to the center angle CA3 or CA4, it indicates that a collision may occur when sailing along the current velocity direction, and the DVOI value is the ratio of CA1 or CA2 to  $\delta$  (depending on which area is closer); When it falls in the area corresponding to the center angle CA5, it indicates that no collision will occur when sailing in the current direction; thus, the DVOI value is 0. The value of DVOI can be calculated according to Equation (12).

$$DVOI = \begin{cases} 1 & \delta \in \{CA1, CA2\} \\ \frac{CA1}{\delta} & \delta \in CA3 \\ \frac{CA2}{\delta} & \delta \in CA4 \\ 0 & \delta \in CA5 \end{cases} \quad (12)$$

### 2.3. Calculation of TVOI

TVOI is the time required for our ship to invade the velocity obstacle cone of the target ship. When the DVOI value is less than 1, this value represents the time when our ship reaches the nearest point to the target ship. When DVOI equals 0, TVOI equals  $+\infty$ . When the relative velocity falls on the velocity obstacle cone, the time of intruding into the velocity obstacle cone of the target ship can be calculated. When the relative velocity falls on the extended cone of the velocity obstacle, the time when our ship reaches the nearest point to the target ship can be calculated.

In Figure 7, the black line indicates the ship’s heading, the yellow arrow indicates the relative heading, and the green dotted line indicates the connection between the center of our ship and the target ship. The collision track of all vertices of our ship against the target ship was determined, as indicated by the red line in Figure 7a. The collision track of all vertices of the target ship against our ship was determined, as shown by the blue line in Figure 7b. The minimum value of all red and blue lines, which is the shortest distance  $D_{min}$  of the intrusion velocity obstacle cone, was calculated. The value of TVOI was  $D_{min}/v_r$ , where  $v_r$  denotes the relative speed of two ships.

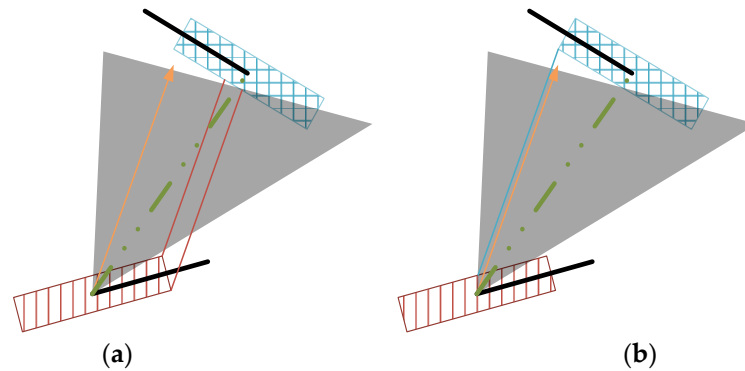


**Figure 7.** Time of invading the velocity obstacle cone. (a) The collision track of vertices of our ship against the target ship. (b) The collision track of a vertex of the target ship against our ship.

When the relative velocity direction was in the extended velocity obstacle cone, we went through the four vertices of our ship, created a straight line parallel to the relative velocity direction, and then calculated the distance from each vertex of the target ship to the straight line, as presented in Figure 8. Among the 16 calculated distances, the vertex of the target ship with the smallest corresponding distance was the point closest to our ship during the voyage, and the perpendicular foot from this point to the corresponding straight line was the nearest point (the intersection of the purple dotted line and the red dotted line). The length of the nearest fixed-point track (i.e., purple dotted line in the figure) from our ship to the target ship was  $d_{min}$ . The value of TVOI was  $d_{min}/v_r$ . Equation (13) was used to calculate TVOI.

$$TVOI = \begin{cases} \frac{D_{min}}{V_r} & \delta \in \{CA1, CA2\} \\ \frac{d_{min}}{V_r} & \delta \in \{CA3, CA4\} \\ 0 & \delta \in CA5 \end{cases} \quad (13)$$

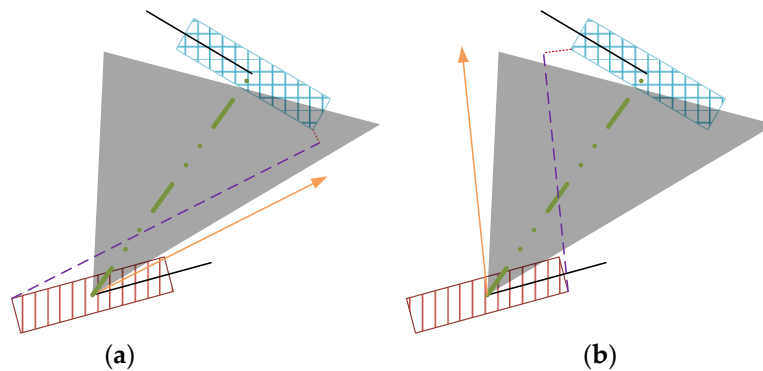


**Figure 8.** Time to the nearest point. (a) From the stern of the target ship to the closest point. (b) From the bow of the target ship to the closest point.

### 3. Pareto Selection Algorithm and Trajectory Compression Filtering

#### 3.1. Pareto Selection Algorithm

DVOI and TVOI evaluate the collision risk from two aspects; thus, a single optimal solution may not be available for the optimal selection of multiple objectives but a set of alternative solutions, called the Pareto solution set [39,40]. Using the algorithm in Algorithm 2, we can obtain the Pareto Frontier of collision risk, which targets our ship's  $1/DVOI$  and TVOI against the target ship. First, exceptional circumstances need to be excluded. When one of the two indicators that a ship evaluates is too large, it generally does not pose a threat to our ship. To exclude this special case, threshold values are specified

for each of the two indicators, and the size of the threshold can be determined based on the channel characteristics or experience. When a ship’s evaluation criteria exceed the threshold, it is not included in the Pareto sorting, as shown in the green area in Figure 9. Although the TVOI value of  $P_F$  and the  $1/DVOI$  value of  $P_G$  were the smallest, these two points still could not dominate other points. The points below the threshold, that is, the red area in Figure 9, were sorted to obtain the first Pareto front.  $P_A$  and  $P_B$  could not be completely dominated, whereas  $P_C$ ,  $P_D$ , and  $P_E$  were completely dominated.

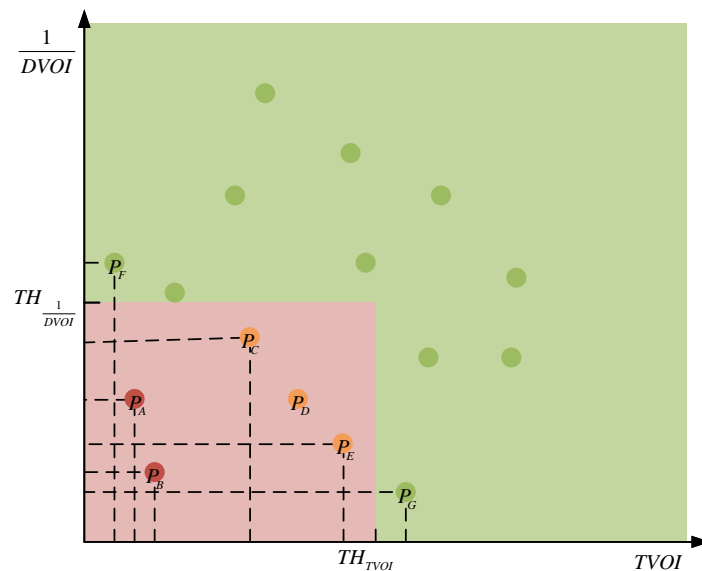


Figure 9. Diagram of the Pareto selection algorithm with a threshold.

Algorithm 2. Algorithm for obtaining the Pareto frontier with a threshold.

**Algorithm 2:** Get Pareto Frontier

**Input:** shipsVOI(MMSI, DVOI, TVOI), TH

**Output:** VOIFrontier

```

// Get Pareto Frontier
1  i ← 0;
2  foreach shipVOI ∈ shipsVOI do
3    if  $\frac{1}{shipVOI.DVOI} > TH \cdot \frac{1}{DVOI} \vee ship.TVOI > TH.TVOI$  then
4      break;
5    end
6    foreach target ∈ (shipsVOI ∧ not used in shipVOI) do
7      if  $\frac{1}{shipVOI.DVOI} > \frac{1}{target.DVOI} \wedge ship.TVOI > target.TVOI$  then
8        break;
9      end
10   end
11   VOIFrontier(i) ← shipVOI.MMSI;
12   i ← i + 1;
13 end
    
```

3.2. Collision Avoidance Operation Point Screening Based on Piecewise Linear Segmentation

To verify the accuracy of the assessment model, the DVOI and TVOI methods are employed to assess the collision risk of AIS data. Specific routes and segments can be screened using the idea of trajectory compression to accurately determine the collision avoidance operation point. Piecewise Linear Segmentation (PLS) is the most used trajectory compression method [41]. Figure 10 presents a schematic of PLS, taking compression of

two-dimensional spatial coordinates as an example. First, the first point  $T_{begin}$  and last point  $T_{end}$  were connected to obtain the deviation from the point on the track to the line. The point on the track corresponding to the maximum deviation  $D$  was used as the segmentation point. The track was then divided into two segments. The above operation was repeated until the maximum deviation of each segment was less than the given threshold  $\epsilon$ . In this paper, time and heading were taken as compression targets, and appropriate thresholds were set using the algorithm in Algorithm 3 to obtain the collision operation points.

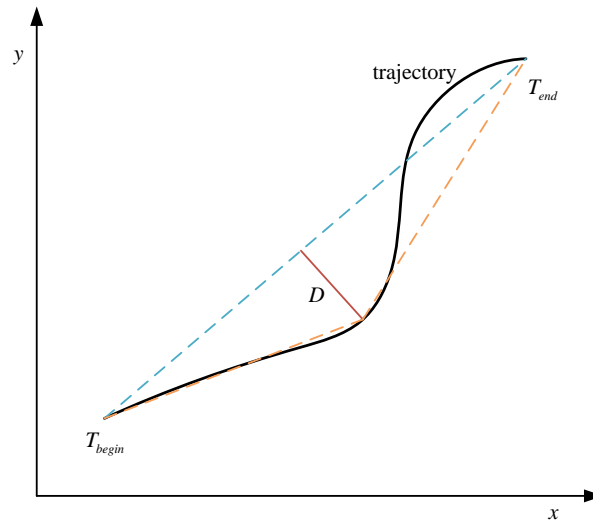


Figure 10. Schematic of PLS.

Algorithm 3. Algorithm for filter segments.

**Algorithm 3:** segmentFilter

**Input:** shipAIS $\epsilon$

**Output:** outshipAIS

```

// Compress the navigation trajectory according to the course threshold
1   $e_{max} \leftarrow 0;$ 
2   $i_{max} \leftarrow 0;$ 
3   $i \leftarrow 2;$ 
4  for  $i \rightarrow end - 1$  do
5  |    $e \leftarrow \text{diff}(\text{shipAIS}(i), \text{Course}, \text{shipAIS}(1), \text{Course}, \text{shipAIS}(end), \text{Course});$ 
6  |   if  $e > e_{max}$  then
7  |   |    $i_{max} \leftarrow i;$ 
8  |   |    $d_{max} \leftarrow d;$ 
9  |   end
10 end
11 if  $d_{max} \geq \epsilon$  then
12 |    $frontPart \leftarrow \text{segmentFilter}(\text{shipAIS}(1, i_{max}), \epsilon);$ 
13 |    $afterPart \leftarrow \text{segmentFilter}(\text{shipAIS}(i_{max}, end), \epsilon);$ 
14 |    $outShipAIS \leftarrow frontPart, afterPart(2, end);$ 
15 else
16 |    $outShipAIS \leftarrow \text{shipAIS}(1), \text{shipAIS}(end);$ 
17 end

```

## 4. Data Processing and Algorithm Flow

### 4.1. AIS Data Preprocessing

Some errors are usually present in the acquired AIS data, which is why the AIS data need to be checked and cleaned up before use [42]. The errors in AIS mainly include

information loss and the information drift [17]. The error criteria for clearing data in this article were as follows:

- Missing ship position, course, speed, length, width and timestamp
- Fewer than three AIS data records
- The speed is lower than 1 knot
- The heading difference of adjacent points is greater than  $50^\circ$
- The track direction change is greater than  $100^\circ$

This paper takes the navigation information of the Jiujiang segment of the Yangtze River basin as an example to obtain AIS data with a time range between 18:30:39 and 23:44:58 (UTC+08:00 as the standard time, the same below) and a geographic range between 116.24–116.35 E and 29.77–29.84 N. The original track obtained is presented in Figure 11a, and the ship track obtained through data cleaning is presented in Figure 11b.

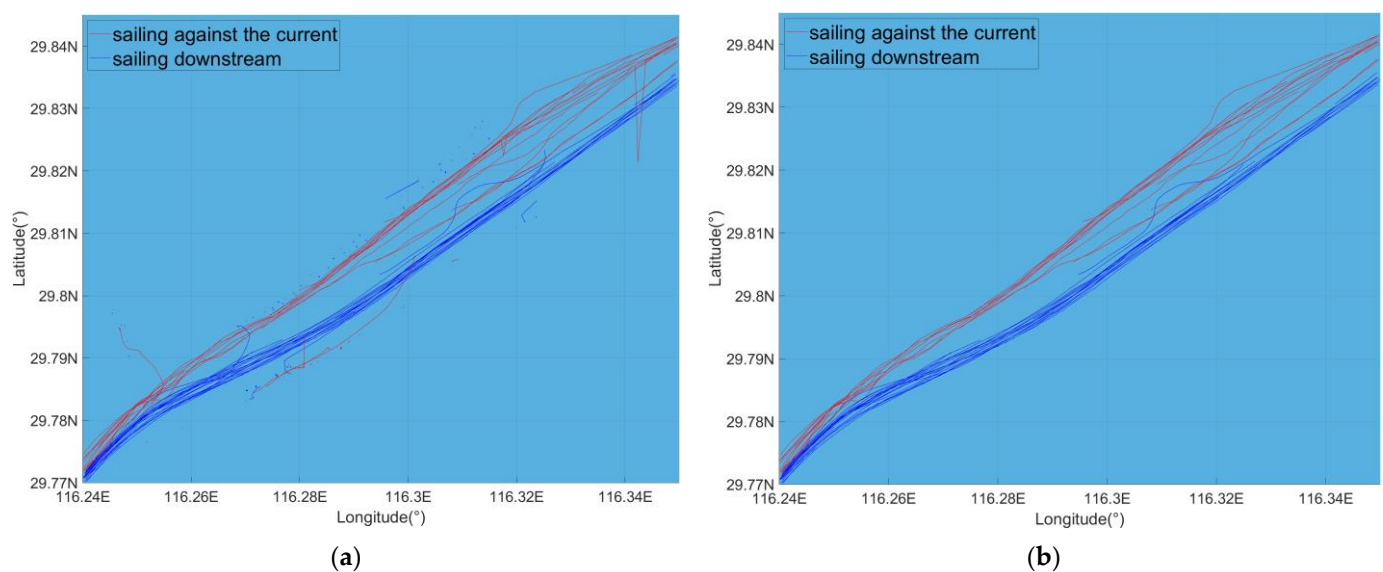


**Figure 11.** Comparison of AIS data before (a) and after (b) cleaning.

#### 4.2. Screening Collision Avoidance Operation Points

In order to verify the effectiveness of the risk assessment function, it was necessary to use the function in the course-keeping and collision avoidance scenarios, respectively. The PLS algorithm introduced in Section 3 was used to screen collision avoidance scenarios. AIS data information was compressed with time and course as the compression target. Figure 12 presents the navigation information of the ship with MMSI No. 413766971 during 27 April 2022 22:17:26 to 27 April 2022 22:34:50. Figure 12a presents the position information. The compressed track points were all turning points with large amplitudes, which can be considered points for the collision avoidance operation. To display the data before and after compression more intuitively, time and heading are taken as the coordinate axis in Figure 12b.

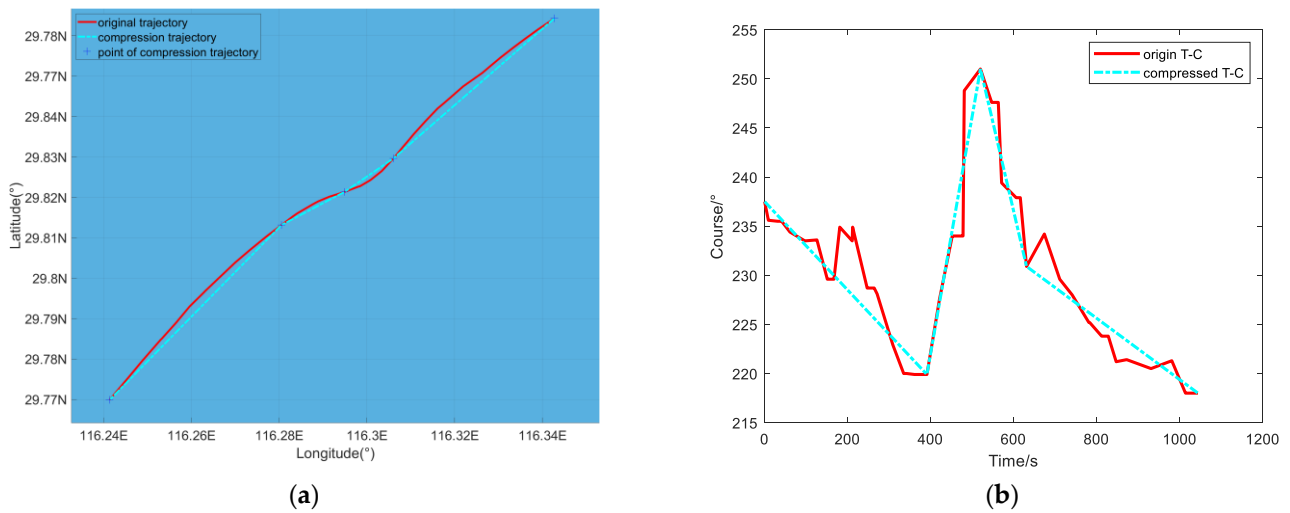


**Figure 12.** AIS data before and after compression. (a) Before and after comparison of track positions. (b) Time-Heading before and after compression.

4.3. Algorithm Flow

As shown in the Figure 13, the algorithm first determines whether the edge collision point needs to be obtained by rotating the coordinate system according to the input AIS information. Then, we calculated the velocity obstacle cone and the extended velocity obstacle cone through the obtained edge collision points, and then we obtained the DVOI. According to whether the value of DVOI was 1, different algorithms were used to obtain TVOI. Finally, through Pareto selection, we obtained the ship with the largest possible collision, and output DVOI and TVOI at the same time.

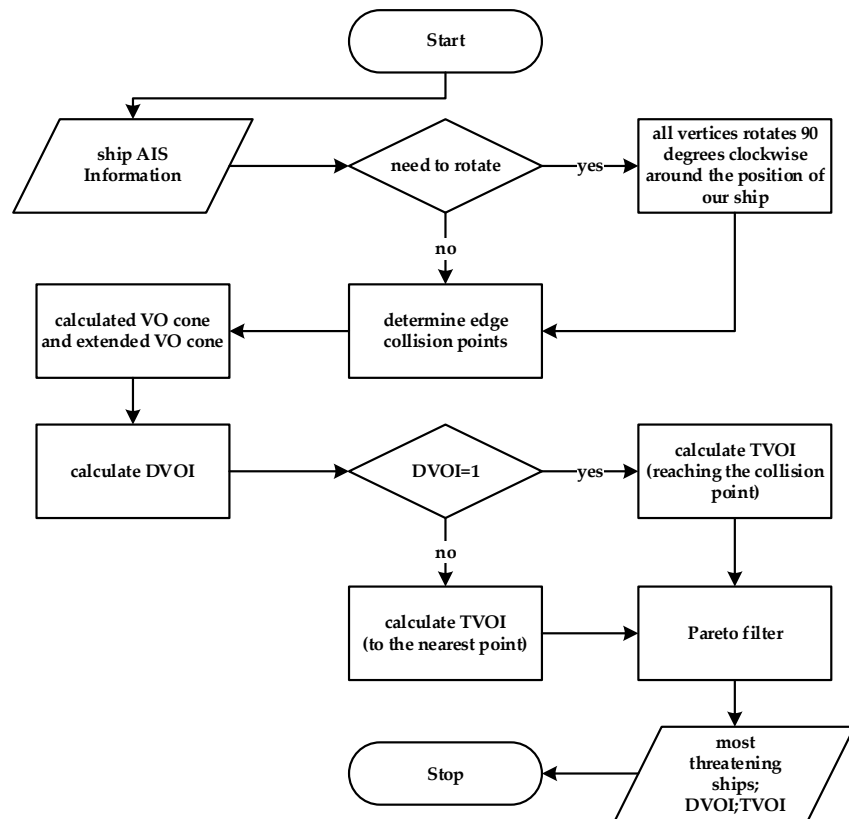


**Figure 13.** The main steps of the algorithm.

### 5. Results and Discussion

When verifying the collision risk assessment model, we selected a ship as our ship, and then used the DVOI/TVOI and CPA methods to assess the collision risk between our ship and the target ships. The sampling frequency of AIS data of different ships is different; thus, the linear interpolation method was employed to obtain the information of target ships at the same time as our ship. The following four cases were all taken from the AIS data of ships in the Jiujiang section of the Yangtze River on 27 April 2022.

#### 5.1. Case 1

The AIS data of two ships with MMSI codes 413762187 and 413826629 at the timestamp 1651070320 (27 April 2022 22:38:40) were acquired, and the navigation collision risk at that time was evaluated using two methods. The AIS data of the two ships at this moment is presented in Table 2.

Table 2. AIS data of Case 1.

MMSI	Longitude (°)	Latitude (°)	Course (°)	Speed (knot)	Length(m)	Width (m)	Heading (°)
413762187	116.3483	29.8408	243.6	4.2	96	15	243.6
413826629	116.3495	29.8403	239.8	4.0354	110	20	239.8

A velocity obstacle cone presented in Figure 14 was constructed, where (a) presents the absolute velocity obstacle cone used to calculate DVOI, (b) shows the relative velocity obstacle cone used to calculate TVOI, and (c) shows the CPA method to calculate DCPA and TCPA. The results are presented in Table 3.

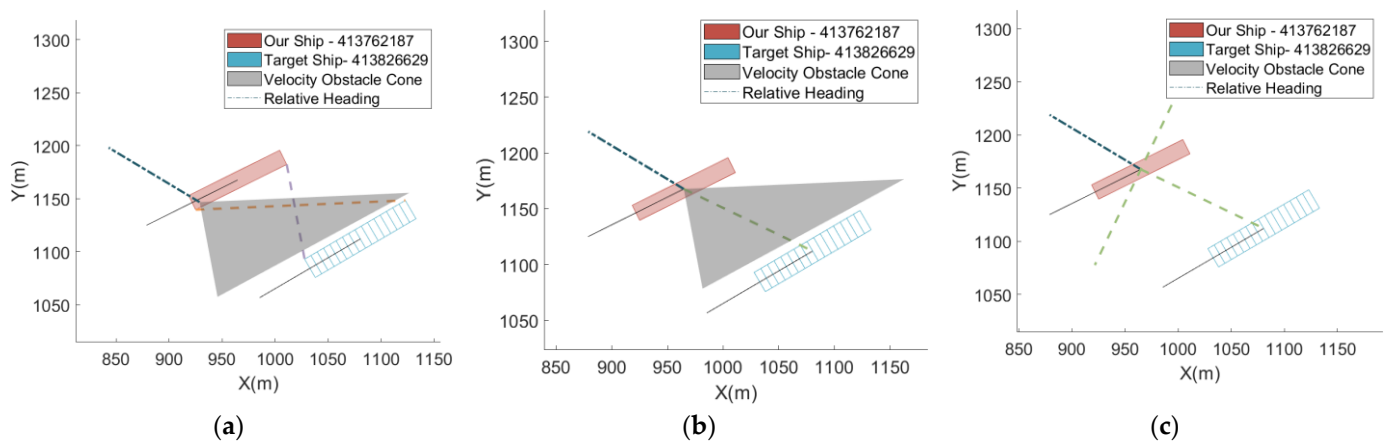


Figure 14. Comparison of DVOI/TVOI and CPA in Case 1. (a) The absolute velocity obstacle cone used to calculate DVOI, (b) the relative velocity obstacle cone used to calculate TVOI, (c) used to calculate DCPA and TCPA.

Table 3. Risk assessment results of Case 1.

DVOI	TVOI (s)	DCPA (m)	TCPA (s)
0	+∞	128.42	0

This scenario is a common situation in inland rivers where two ships navigate side by side. At this point, because the relative course of the two ships is outside the extended velocity obstacle cone, the DVOI value is 0, i.e., the two ships will never collide when traveling in their current state. The value of DCPA is 128.42. The threshold of DCPA (double the sum of the lengths of two vessels) is usually greater than this value, and the CPA method is liable to cause a false alarm (early alarm).

5.2. Case 2

The AIS data of two ships with MMSI codes 41372187 and 413158879 with timestamp 1651070520 (27 April 2022 22:42:00) were obtained, and collision risk at that time was assessed using two methods. The AIS data of the two ships at this time are presented in Table 4.

Table 4. AIS data of Case 2.

MMSI	Longitude (°)	Latitude (°)	Course (°)	Speed (knot)	Length(m)	Width (m)	Heading (°)
413762187	116.3436	29.8387	239.4	4.4	96	15	239.4
413815879	116.3387	29.8354	236.7	3.7	59	11	236.7

The velocity obstacle cone was constructed as shown in Figure 15, and the results of the collision risk assessment are presented shown in Table 5.

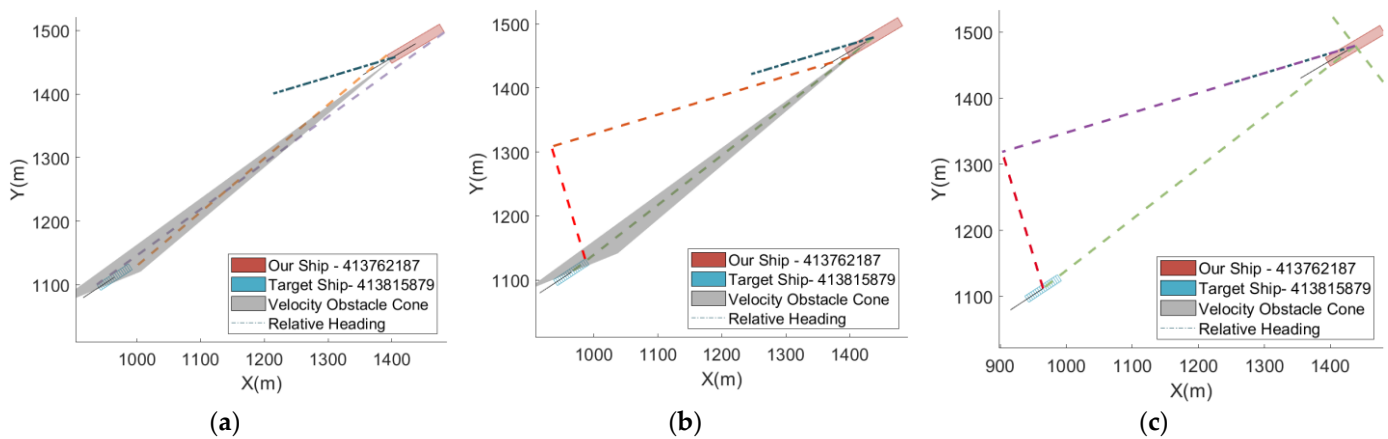


Figure 15. Comparison of DVOI/TVOI and CPA in Case 2. (a) The absolute velocity obstacle cone used to calculate DVOI, (b) the relative velocity obstacle cone used to calculate TVOI, (c) used to calculate DCPA and TCPA.

Table 5. Risk assessment results of Case 2.

DVOI	TVOI (s)	DCPA (m)	TCPA (s)
0.09	1304.38	215.72	1495.96

The scenario is a common sailing scenario in the inner river, where one ship follows the other ship. The CPA method ignores the ships' size. TCPA can only act as the collision time when DCPA is less than the threshold. When DCPA is slightly larger than the threshold, TCPA lacks reference and is difficult to use in judging the current sailing collision risk. However, the extent of the relative heading away from the velocity obstacle cone can be judged from the DVOI values using the DVOI/TVOI method. DVOI = 0.09, which is much less than 1 at a certain collision. From the DVOI calculation method, a sufficiently safe approach at this time is to relatively navigate away from the velocity obstacle cone at an angle about 10 times that of the velocity obstacle cone and with a TVOI value of 1304.38 s. This case shows that the DVOI/TVOI method covers more information than the CPA method and can avoid premature alarms and false alarms by increasing unnecessary redundancy due to security considerations in the CPA method.

5.3. Case 3

To obtain AIS data for two vessels with MMSI codes 413773475 and 413839828 poked at time 1651073819 (27 April 2022 23:36:59) and to evaluate the sailing collision risk at that

moment using the two methods, the AIS data of two vessels at the moment are presented in Table 6.

**Table 6.** AIS data of Case 3.

MMSI	Longitude (°)	Latitude (°)	Course (°)	Speed (knot)	Length(m)	Width (m)	Heading (°)
413773475	116.2580	29.7855	73.1	5.5	110	19	73.1
413839828	116.2541	29.7810	58.4	7.8	130	16	36.8

The velocity obstacle zone was constructed as presented in Figure 16, and the results of the collision risk assessment are shown in Table 7.

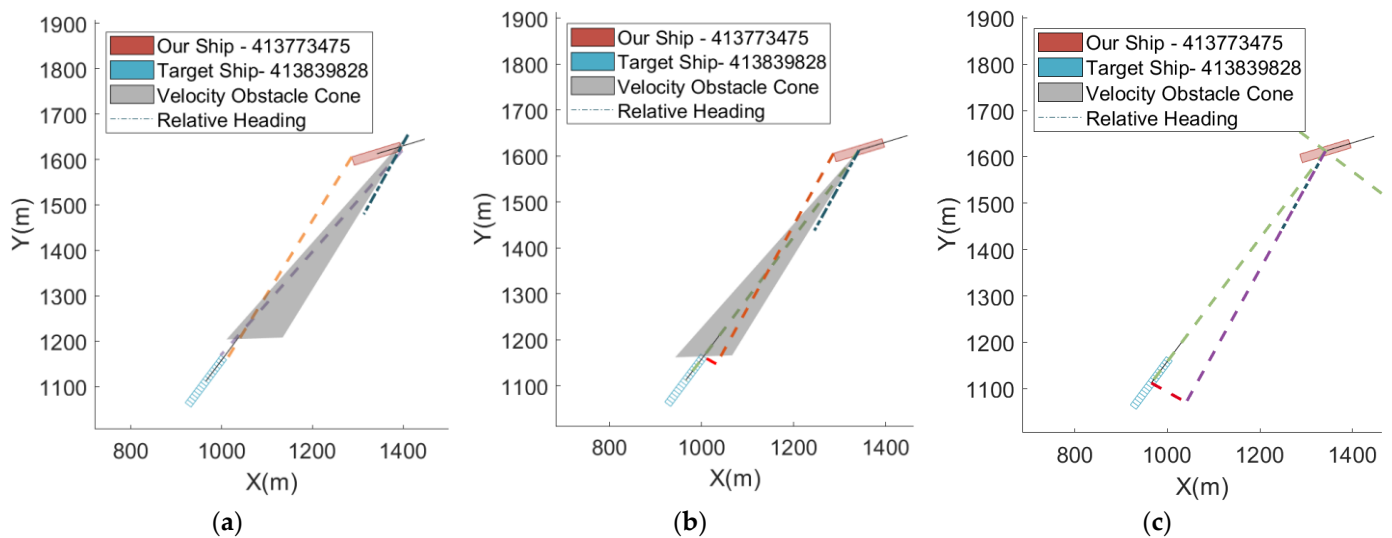


**Figure 16.** Comparison of DVOI/TVOI and CPA in Case 3. (a) The absolute velocity obstacle cone used to calculate DVOI, (b) the relative velocity obstacle cone used to calculate TVOI, (c) used to calculate DCPA and TCPA.

**Table 7.** Risk assessment results of Case 3.

DVOI	TVOI (s)	DCPA (m)	TCPA (s)
0.66	357.95	86.28	423.69

The scenario is the crossing of a ship in the inner river from the front of another ship, at which time both the DVOI and DCPA values indicated that the scenario was more dangerous, but the value of TVOI was 65.74 s less than that of TCPA. This result occurred because the CPA method does not take into account the size factor of vessels. Thus, the calculated results can sometimes be smaller than the actual collision risk value, resulting in an insufficient warning. Meanwhile, the TVOI was calculated considering the vessel size, and the results were more precise.

5.4. Case 4

All ships' AIS data with timestamp 1651069257 (27 April 2022 22:20:57) in the range 116.246–116.262 East and 29.779–29.792 north were acquired, and the data are presented in Table 8.

**Table 8.** AIS data of Case 4.

MMSI	Longitude (°)	Latitude (°)	Course (°)	Speed (knot)	Length(m)	Width (m)	Heading (°)
413766971	116.2605	29.7895	233.5	5.8	75	13	233.5
413832087	116.2559	29.7840	218.6	3.7	83	14	218.6
413828271	116.2533	29.7841	234.4	5.4	114	19	234.4
413793803	116.2533	29.7833	38.4	5.3	81	14	38.4
413796206	116.2493	29.7815	215.0	4.9	93	16	214.3
413798243	116.2484	29.7903	74.4	0	86	14	0

The ship with MMSI number 413766971 was selected as our ship, and the collision risk was calculated for the rest of the ships. The relative positions of each ship are shown in Figure 17. The calculation results of DVOI and TVOI are presented in Table 9. Pareto ordering of the above vessels was performed using 1/DVOI and TVOI, of which 413828271 was significantly outside the threshold and did not participate in the Pareto frontier ordering. The Pareto frontier graph is presented in Figure 18. Figure 18 demonstrates that the ship with MMSI number 41373803 had the greatest risk to our ship, that is, the ship represented by the five-point star in Figure 18.

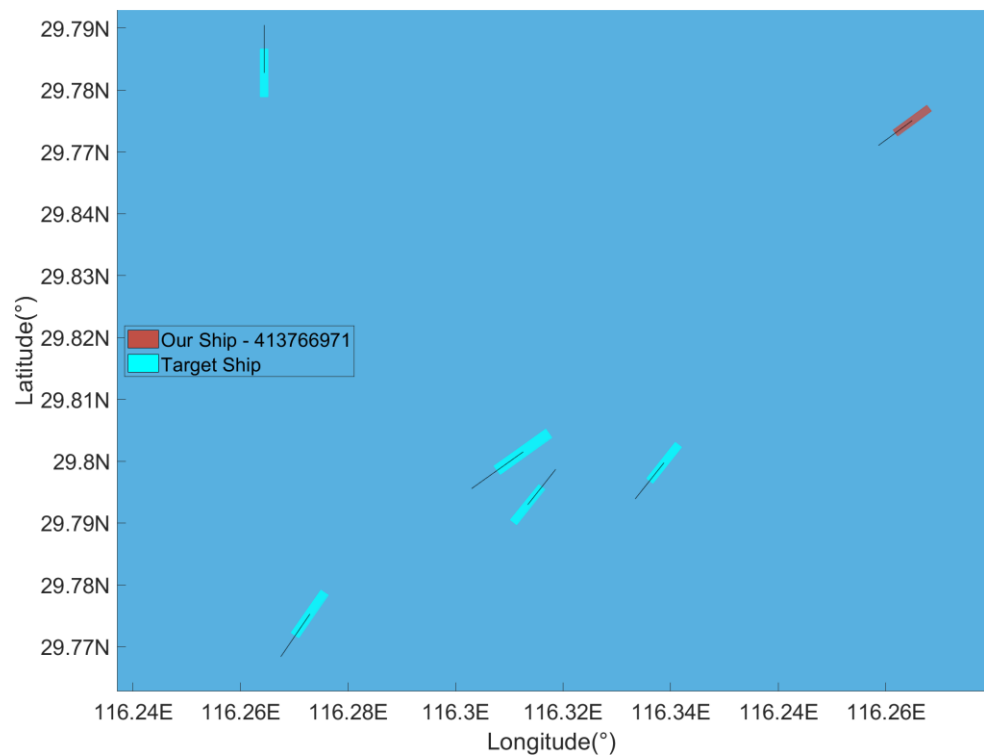


**Figure 17.** Relative position of each ship in Case 4.

**Table 9.** Risk assessment results of Case 4.

MMSI	DVOI	TVOI (s)	1/DVOI
413832087	0.04	413.98	25
413828271	0.18	4055.41	5.5
413793803	1	169.45	1
413796206	0.02	754.05	50
413798243	0.09	294.98	11.1

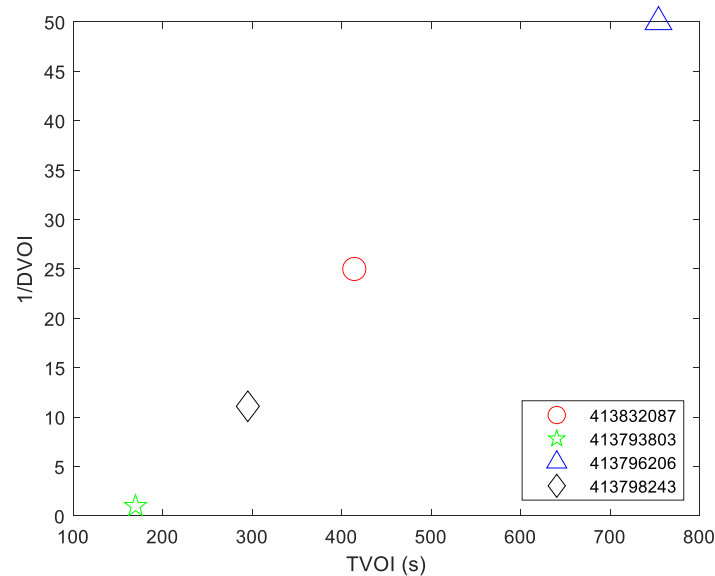


**Figure 18.** Pareto ranking of ship risk indicators in Case 4.

### 5.5. Summary

Case 1 shows that when two ships are sailing side by side, the DVOI/TVOI method is more accurate than the CPA method, which prevents the premature alarm caused by an overly large DCPA threshold in the CPA.

Case 2 is a case in which the DVOI/TVOI method covers more information than the CPA method during the two-vessel chase voyage, making up for the lack of referential TCPA in the CPA.

Case 3 is a case in which the DVOI/TVOI method is more accurate than the CPA method when the two ships are crossing. The CPA method ignores the size information of the ship itself, resulting in an insufficient early warning.

Case 4 is a case in which DVOI/TVOI is combined with Pareto selection to identify the vessel that poses the greatest threat to a vessel under multivessel navigation.

## 6. Conclusions

In this paper, a method for real-time detection of collision risk of inland navigation was presented, which was combined with the velocity obstacle method and Pareto selection to solve the problem of the existing inland navigation collision risk model being unsuitable for the inland river environment. This method included a real-time collision risk assessment model based on AIS data of the ships' size and the velocity obstacle method, as well as a Pareto selection algorithm with thresholds. In the collision risk assessment model, a method for constructing a velocity obstacle cone for a convex polygon was presented, and two collision risk assessment indices—DVOI and TVOI—were defined to evaluate the collision risk of navigation from the aspects of course and speed. Then, the Pareto selection algorithm with threshold was employed to combine the risk information of two dimensions to determine which ship poses the greatest threat to our ship in the current course state. This feature is especially important for choosing the collision avoidance order when multivessel collisions need to be avoided. The real AIS historical data were used to assess collision risk in navigation scenarios such as side-by-side, overtaking, and cross-navigation. The experiment results were compared with those of typical CPA methods and showed that the results of the DVOI/TVOI methods contained more information and were more accurate than those of the CPA methods.

To verify the reliability of DVOI/TVOI collision risk assessment models in various scenarios, the scenarios that contain ship collision avoidance operations need to be filtered accurately from the AIS data. In this paper, an AIS error data clearing method was presented,

and a method for filtering AIS data containing ship collision avoidance scenario data was presented using the PLS algorithm with time and course as the compression target.

Compared with the CPA method, the collision assessment method proposed in this paper solves the problem that CPA cannot effectively assess the navigation collision risk in restricted waters such as inland rivers. This method can accurately evaluate the risk of two ships side by side or encountering at close range and is more accurate than the CPA method for overtaking and crossing situations. This is of great significance to the ship-assisted collision avoidance and intelligent navigation of inland ships. The proposal of this method is beneficial for ship path planning or the collision avoidance decision-making algorithm to determine the timing of collision avoidance and resumption of the voyage more reasonably. The crew or decision-making algorithms can prioritize collision avoidance targets based on quantified collision risk values, which will greatly reduce collisions due to human error. According to the quantified value of collision risk, a hierarchical and classified navigation decision-making response algorithm can be developed to improve the flexibility of the navigation decision-making module. Moreover, the evaluation method can also be used as a new index to be applied to the metaheuristic algorithm to improve the accuracy and reliability of the existing inland ship collision avoidance scheme. In addition to applications for ship-assisted collision avoidance or the intelligent navigation of ships in inland waterways, DVOI/TVOI, as a brand-new collision risk assessment index, can also be applied to various analysis methods. For example, by analyzing a large amount of AIS data, the collision risk value threshold range of a given segment can be determined to obtain the regional risk value. This can provide more useful information for vessel traffic service operators (VTSO).

**Author Contributions:** Conceptualization, Y.W. and H.W.; methodology, Y.W.; software, Y.W.; validation, Y.Z., H.Z. and H.W.; formal analysis, Y.W.; investigation, Y.Z.; resources, H.Z.; data curation, H.Z.; writing—original draft preparation, Y.W.; writing—review and editing, H.W.; visualization, Y.W.; supervision, H.W.; project administration, H.W.; funding acquisition, H.W. All authors have read and agreed to the published version of the manuscript.

**Funding:** This research was funded by National Natural Science Foundation of China, grant number U1964202.

**Institutional Review Board Statement:** Not applicable.

**Informed Consent Statement:** Not applicable.

**Data Availability Statement:** Not applicable.

**Conflicts of Interest:** The authors declare no conflict of interest.

## References

1. Qian, L.; Zheng, Y.Z.; Li, L.; Ma, Y.; Zhou, C.H.; Zhang, D.F. A New Method of Inland Water Ship Trajectory Prediction Based on Long Short-Term Memory Network Optimized by Genetic Algorithm. *Appl. Sci.* **2022**, *12*, 4073. [[CrossRef](#)]
2. Zhang, G.Y.; Wang, Y.; Liu, J.; Cai, W.; Wang, H.B. Collision-Avoidance Decision System for Inland Ships Based on Velocity Obstacle Algorithms. *J. Mar. Sci. Eng.* **2022**, *10*, 814. [[CrossRef](#)]
3. Chauvin, C.; Lardjane, S.; Morel, G.; Clostermann, J.P.; Langard, B. Human and organisational factors in maritime accidents: Analysis of collisions at sea using the HFACS. *Accid. Anal. Prev.* **2013**, *59*, 26–37. [[CrossRef](#)]
4. Graziano, A.; Teixeira, A.P.; Guedes Soares, C. Classification of human errors in grounding and collision accidents using the TRACER taxonomy. *Saf. Sci.* **2016**, *86*, 245–257. [[CrossRef](#)]
5. Pedersen, P.T. Review and application of ship collision and grounding analysis procedures. *Mar. Struct.* **2010**, *23*, 241–262. [[CrossRef](#)]
6. Zhang, M.Y.; Zhang, D.; Yao, H.J.; Zhang, K. A probabilistic model of human error assessment for autonomous cargo ships focusing on human-autonomy collaboration. *Saf. Sci.* **2020**, *130*, 104838. [[CrossRef](#)]
7. Huang, Y.; Chen, L.; Chen, P.; Negenborn, R.R.; van Gelder, P.H.A.J.M. Ship collision avoidance methods: State-of-the-art. *Saf. Sci.* **2020**, *121*, 451–473. [[CrossRef](#)]
8. Liu, Z.H.; Wu, Z.L.; Zheng, Z.Y. A novel framework for regional collision risk identification based on AIS data. *Appl. Ocean Res.* **2019**, *89*, 261–272. [[CrossRef](#)]
9. Kang, L.J.; Meng, Q.; Liu, Q. Fundamental diagram of ship traffic in the Singapore Strait. *Ocean Eng.* **2018**, *147*, 340–354. [[CrossRef](#)]

10. Mou, J.M.; van der Tak, C.; Ligteringen, H. Study on collision avoidance in busy waterways by using AIS data. *Ocean Eng.* **2010**, *37*, 483–490. [[CrossRef](#)]
11. Kang, L.J.; Lu, Z.Y.; Meng, Q.; Gao, S.; Wang, F.W. Maritime simulator based determination of minimum DCPA and TCPA in head-on ship-to-ship collision avoidance in confined waters. *Transp. A* **2019**, *15*, 1124–1144. [[CrossRef](#)]
12. Szlapczynski, R.; Szlapczynska, J. Review of ship safety domains: Models and applications. *Ocean Eng.* **2017**, *145*, 277–289. [[CrossRef](#)]
13. Szlapczynski, R. A unified measure of collision risk derived from the concept of a ship domain. *J. Navig.* **2006**, *59*, 477–490. [[CrossRef](#)]
14. Szlapczynski, R.; Szlapczynska, J. An analysis of domain-based ship collision risk parameters. *Ocean Eng.* **2016**, *126*, 47–56. [[CrossRef](#)]
15. Qiao, Z.X.; Zhang, Y.J.; Wang, S.B. A Collision Risk Identification Method for Autonomous Ships Based on Field Theory. *IEEE Access* **2021**, *9*, 30539–30550. [[CrossRef](#)]
16. Namgung, H.; Kim, J.S. Regional Collision Risk Prediction System at a Collision Area Considering Spatial Pattern. *J. Mar. Sci. Eng.* **2021**, *9*, 1365. [[CrossRef](#)]
17. Lei, J.; Liu, L.; Chu, X.; He, W.; Liu, X.; Liu, C. Automatic identification system data-driven model for analysis of ship domain near bridge-waters. *J. Navig.* **2021**, *74*, 1284–1304. [[CrossRef](#)]
18. Rong, H.; Teixeira, A.P.; Soares, C.G. Ship trajectory uncertainty prediction based on a Gaussian Process model. *Ocean Eng.* **2019**, *182*, 499–511. [[CrossRef](#)]
19. Chen, P.; Huang, Y.; Mou, J.; van Gelder, P.H.A.J.M. Ship collision candidate detection method: A velocity obstacle approach. *Ocean Eng.* **2018**, *170*, 186–198. [[CrossRef](#)]
20. Zhou, J.; Wang, C.; Zhang, A. A COLREGs-Based Dynamic Navigation Safety Domain for Unmanned Surface Vehicles: A Case Study of Dolphin-I. *J. Mar. Sci. Eng.* **2020**, *8*, 264. [[CrossRef](#)]
21. Wang, N. An Intelligent Spatial Collision Risk Based on the Quaternion Ship Domain. *J. Navig.* **2010**, *63*, 733–749. [[CrossRef](#)]
22. Liu, Z.H.; Wu, Z.L.; Zheng, Z.Y. A cooperative game approach for assessing the collision risk in multi-vessel encountering. *Ocean Eng.* **2019**, *187*, 12. [[CrossRef](#)]
23. Liu, Z.H.; Wu, Z.L.; Zheng, Z.Y. A Collision Avoidance Manoeuvre and Ship Domain Based Model for Identifying Collision Risk Index between Ships. In Proceedings of the 4th Annual International Conference on System Reliability and Safety (ICSRS), Rome, Italy, 20–22 November 2019; pp. 255–261.
24. You, Y.J.; Rhee, K. Development of the collision ratio to infer the time at which to begin a collision avoidance of a ship. *Appl. Ocean Res.* **2016**, *60*, 164–175. [[CrossRef](#)]
25. Li, J.; Wang, H.; Guan, Z.; Pan, C. Distributed Multi-Objective Algorithm for Preventing Multi-Ship Collisions at Sea. *J. Navig.* **2020**, *73*, 971–990. [[CrossRef](#)]
26. Chen, P.F.; Li, M.X.; Mou, J.M. A Velocity Obstacle-Based Real-Time Regional Ship Collision Risk Analysis Method. *J. Mar. Sci. Eng.* **2021**, *9*, 428. [[CrossRef](#)]
27. Guan, Z.; Wang, Y.; Zhou, Z.; Wang, H. Research on Early Warning of Ship Danger Based on Composition Fuzzy Inference. *J. Mar. Sci. Eng.* **2020**, *8*, 1002. [[CrossRef](#)]
28. Ahn, J.H.; Rhee, K.P.; You, Y.J. A study on the collision avoidance of a ship using neural networks and fuzzy logic. *Appl. Ocean Res.* **2012**, *37*, 162–173. [[CrossRef](#)]
29. Zhao, Y.X.; Li, W.; Shi, P. A real-time collision avoidance learning system for Unmanned Surface Vessels. *Neurocomputing* **2016**, *182*, 255–266. [[CrossRef](#)]
30. Li, B.; Pang, F.W. An approach of vessel collision risk assessment based on the D-S evidence theory. *Ocean Eng.* **2013**, *74*, 16–21. [[CrossRef](#)]
31. Kaneko, F. Methods for probabilistic safety assessments of ships. *J. Mar. Sci. Technol.* **2002**, *7*, 1–16. [[CrossRef](#)]
32. Yu, Q.; Liu, K.; Chang, C.-H.; Yang, Z. Realising advanced risk assessment of vessel traffic flows near offshore wind farms. *Reliab. Eng. Syst. Saf.* **2020**, *203*, 1–16. [[CrossRef](#)]
33. Li, K.X.; Yin, J.B.; Bang, H.S.; Yang, Z.L.; Wang, J. Bayesian network with quantitative input for maritime risk analysis. *Transp. A* **2014**, *10*, 89–118. [[CrossRef](#)]
34. Cai, M.; Zhang, J.; Zhang, D.; Yuan, X.; Soares, C.G. Collision risk analysis on ferry ships in Jiangsu Section of the Yangtze River based on AIS data. *Reliab. Eng. Syst. Saf.* **2021**, *215*, 107086. [[CrossRef](#)]
35. Mujeeb-Ahmed, M.P.; Paik, J.K. A probabilistic approach to determine design loads for collision between an offshore supply vessel and offshore installations. *Ocean Eng.* **2019**, *173*, 358–374. [[CrossRef](#)]
36. Tu, E.M.; Zhang, G.H.; Rachmawati, L.; Rajabally, E.; Huang, G.B. Exploiting AIS Data for Intelligent Maritime Navigation: A Comprehensive Survey From Data to Methodology. *IEEE Trans. Intell. Transp. Syst.* **2018**, *19*, 1559–1582. [[CrossRef](#)]
37. Qu, X.B.; Meng, Q.; Li, S.Y. Ship collision risk assessment for the Singapore Strait. *Accid. Anal. Prev.* **2011**, *43*, 2030–2036. [[CrossRef](#)] [[PubMed](#)]
38. Fiorini, P.; Shiller, Z. Motion Planning in Dynamic Environments Using Velocity Obstacles. *Int. J. Robot. Res.* **1998**, *17*, 760–772. [[CrossRef](#)]
39. Yang, S.X.; Li, M.Q.; Liu, X.H.; Zheng, J.H. A Grid-Based Evolutionary Algorithm for Many-Objective Optimization. *IEEE Trans. Evol. Comput.* **2013**, *17*, 721–736. [[CrossRef](#)]

40. Li, M.Q.; Yang, S.X.; Liu, X.H. Pareto or Non-Pareto: Bi-Criterion Evolution in Multiobjective Optimization. *IEEE Trans. Evol. Comput.* **2016**, *20*, 645–665. [[CrossRef](#)]
41. de Vries, G.K.D.; van Someren, M. Machine learning for vessel trajectories using compression, alignments and domain knowledge. *Expert Syst. Appl.* **2012**, *39*, 13426–13439. [[CrossRef](#)]
42. Kang, L.J.; Meng, Q.; Zhou, C.B.; Gao, S. How do ships pass through L-shaped turnings in the Singapore strait? *Ocean Eng.* **2019**, *182*, 329–342. [[CrossRef](#)]